Hindawi
Adsorption Science & Technology
Volume 2022, Article ID 4112448, 19 pages
https://doi.org/10.1155/2022/4112448

Research Article

Comparative Study on EDM Parameter Optimization for Adsorbed Si_3N_4–TiN using TOPSIS and GRA Coupled with TLBO Algorithm

V. P. Srinivasan,[1] **Ch. Sandeep**,[2] **C. Shanthi**,[3] **A. Bovas Herbert Bejaxhin**,[4] **R. Anandan**,[5] **and M. Abisha Meji**[6]

[1]*Department of Mechanical Engineering, Sri Krishna College of Engineering and Technology, 641 008, Coimbatore, Tamil Nadu, India*
[2]*Department of Mechanical Engineering, Institute of Aeronautical Engineering, 500 043, Hyderabad, Telangana, India*
[3]*Department of Physics, Sona College of Technology, 636 005, Salem, Tamil Nadu, India*
[4]*Department of Mechanical Engineering, Saveetha School of Engineering, SIMATS, 602 105, Chennai, Tamil Nadu, India*
[5]*Department of Mechanical Engineering, Vinayaka Mission's Kirupananda Variyar Engineering College, Vinayaka Mission's Research Foundation, Deemed to be University, 636 308, Salem, Tamil Nadu, India*
[6]*School of Engineering and Applied Sciences, Kampala International University, Western Campus, Uganda*

Correspondence should be addressed to V. P. Srinivasan; vpsrinivasa@gmail.com and M. Abisha Meji; abisha.meji@kiu.ac.ug

Received 26 July 2022; Accepted 12 September 2022; Published 30 September 2022

Academic Editor: Debabrata Barik

Electrical discharge machining is a thermo-physical-based material removal technique. 25 combinations of process variables were formulated with the aid of Taguchi technique for EDM of adsorbed Si_3N_4–TiN. Machining variables like pulse current, pulse-on time, pulse-off time, dielectric pressure, and spark gap voltage varied, and impact of each variables on the performance metrics (MRR, EWR, SR, ROC, θ, CIR, and CYL) was assessed. MCDM strategies like grey relational analysis and TOPSIS are utilized to find out the ideal arrangement of machining parameters to achieve most acute productivity of the multitude of reactions. Likewise, metaheuristic algorithm in particular GRA combined with teaching-learning-based optimization algorithm is utilized for getting global optimized input factors. Important factors like pulse current, pulse-on time, and spark gap voltage characteristically affect the outputs. It is recognized that the pulse-on time and the pulse current are the most significant input factors than others. The ideal machining parameters in view of GRA and TOPSIS techniques for acquiring better output factors are I, 12 amps; PON, 7 μsec; POFF, 4 μsec; DP, 12 kg/cm^2; and SV, 36 volts.

1. Introduction

Thermo-physical-based material removal technique named EDM is a modern machining methodology with phenomenal capacity of noncontact machining of profoundly hard and brittle workpieces with accurate three-dimensional complex shapes. Conceivably, surface attributes of the materials can be altered by the EDM process. The predominant problem associated with electrical discharge machining is a poor surface finish. By employing compacted electrodes, particles during the machining process will be settled on the material surface and limit the microcracks, voids, recast layer, and so forth [1–3]. The electrical discharge machining process guarantees legitimate carbonation and surface heat-treatment, and a superior material hardness was acquired with an elevated peak current and reduced duty factor [4]. The electrodischarge machining of each nonconductive workpiece relies upon large variables. Nickel and carbon intensify structure harmful mixtures like Ni $(CN)_2$ and (C_5H_5) NiNO. Nitrogen-containing ceramic materials (nitrides AlN, SiAlON, and Si_3N_4) are not being handled in hydrocarbons with a nickel holding assistive electrode

[5]. Material transmits by powder metallurgy electrodes and by powder particles suspended in the dielectric liquid; these two techniques offer practical option in contrast to the next right now utilized costly strategies for surface modifications like ion implantation and laser surface processing [6]. Both EDM and powder-mixed EDM can support the deposition of surface layers having novel trademark with unrivaled capability as far as mechanical, metallurgical, and tribological characteristics [7]. To accomplish green and healthy production, save resources, reduce the number of experimental trails, and improve the efficiency of experimental work, CuSn CLEs were employed [8]. Gap-active EDM is another methodology which gives a gap-detectable and automatic adjustable electrode retraction set up to facilitate improved textual attribute with reduced indentation, solidified-agglomerates, and crack [9]. Selecting permissible dielectric fluid is additionally indispensable in EDM since it has influence on the surface roughness. Using water as dielectric fluid advances a safe environment. Also, the electrode wear rate will be less, and surface finish will be better. On the other hand, hydrocarbon oil such as kerosene will break down and deliver harmful vapors like CO and CH_4 during EDM [10]. Also, vegetable oil-based dielectric liquids, namely, sunflower and jatropha oils, have homogeneous dielectric properties and erosion procedure when correlated with the traditional dielectric fluid. For sustainable manufacturing, biodegradable and ecofriendly vegetable oil-based dielectric liquid shall be selected [11]. TLBO algorithm is a novel population-based nature exhilarated breakthrough, and it has two stages specifically "teacher phase" and "learner phase." The modified TLBO technique also has two phases and exploits a new population class system into a traditional TLBO technique. The modified TLBO technique delineates an enhanced result quality and quick intermingling ratio than traditional TLBO. Statistical investigations on the trial results elucidated an extensive performance for proposed changes [12–14]. The TLBO algorithm has an extensive likely when contrasted with the combinatorial optimization complexity, like job-shop scheduling problems and flow-shop scheduling problems [15]. In joint optimization of TLBO, PSO, and GA, TLBO conferred impressive has surpassing amount of combination and within the fixed trails of iterations [16].

Square profiles in silicon nitride–titanium nitride are made using square tungsten-copper electrodes, and the machining input factors like I, PON, POFF, DP, and SV are optimized using various methodologies like GRA, TOPSIS, and GRA coupled with TLBO algorithm [1]. Adsorbed silicon nitride–titanium nitride CMCs are best suited for high temperature applications because of their admirable properties. Contributions by numerous researchers in the area of mechanism of electrical discharge machining, influence of EDM parameters, selection of tool electrode, selection to dielectric fluid, influence of powder particles mixed with dielectric fluid, after machining surface morphology, etc., were considered for identifying the research gap in the previous work. In continuation to the previous work, currently circular profiles are made in silicon nitride–titanium nitride using cylindrical tungsten-copper electrodes, and the machining input factors like I, PON, POFF, DP, and SV are optimized using joint optimization techniques. The response factors like MRR, EWR, SR, ROC, θ, CIR, and CYL are considered. The optimum electrical discharge machining ranges were attained by means of the Taguchi optimization technique for circular profiles. The optimal group of electrical discharge machining factors was attained through MCDM techniques like GRA and TOPSIS. Also, global optimization approach GRA coupled with the TLBO algorithm was preferred. The optimal combination model bestows more prominent anticipated outcomes than estimated.

2. Experimental Procedure

Figure 1 depicts flawless exploration procedure of which the experimental work and electrical discharge machining parameter optimization are done. Commercially available silicon nitride–titanium nitride composites are used as workpiece material for the current research. Usually, silicon nitride–titanium nitride composites are fabricated by hot pressing and SPS process by mixing of Si_3N_4 and Ti powders at 1350°C temperature [17–19]. Si_3N_4–TiN has been selected because of its superior properties like high melting point, increased thermal shock resistance, high strength retention at elevated temperatures, excellent corrosion and wear resistance, improved surface hardness, and low density. It finds extensive applications in wear resistant parts, heat exchangers, gas turbines, extrusion dies, ball bearings, shot blast nozzle, level sensors in molten metal, and aircraft engines parts. In the Si_3N_4–TiN workpiece, electrical discharge machining is led utilizing electronic die-sinker (500×300 series) ED machine. Circular holes of 3 mm diameter are shaped on the Si_3N_4–TiN workpiece which is of 2 mm thickness and 50 mm diameter. The machining process was finished with tungsten-copper (W-Cu) material electrode of 3 mm diameter and 15 mm length. The Si_3N_4–TiN workpiece subsequent to the process is delineated in Figure 2. For every circular pocket, one new cylindrical-shaped electrode was chosen, and the tool electrodes before and after processing are shown in Figures 3(a) and 3(b), respectively. The deionized water is employed as dielectric liquid for safe environment [10].

2.1. Design of Experiments. The design of experiments is an organized way for regulating the correlation in dispersion through input factors impacting the process and output factors of that cycle. DOE facilitates to get convenient data around the process by directing least number of trails. The experimentations were accomplished using five input parameters differed at five positions as shown in Table 1. The DOE with 25 machining run order as obtained from the Taguchi methodology was produced using Minitab 19.0 statistical tool [1]. The order on which the experimental work is carried out and also the time taken for machining is shown in Table 2. The experimental results are portrayed in Table 3.

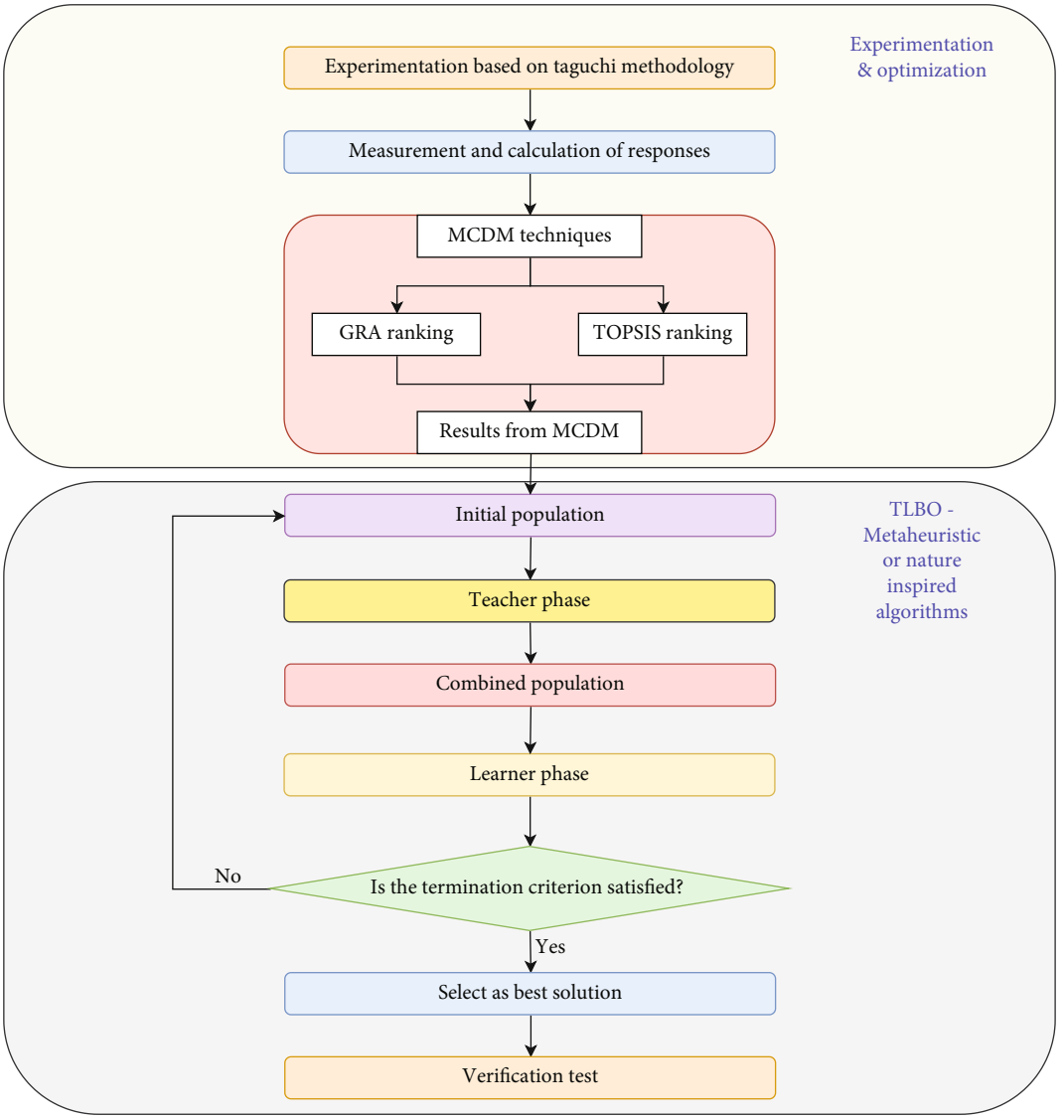

Figure 1: Proposed research plan (Srinivasan et al. [1]).

2.2. Measurements and Calculations of Response Factors. The MRR and the EWR were determined using Equation (1) and Equation (2), respectively. The radial overcut and taper angle were calculated using Equation (3) and Equation (4), respectively.

$$\text{Material removal rate, MRR} = \frac{W_{\text{initial}} - W_{\text{final}}}{\text{MT}}\ (\text{gm/min}), \tag{1}$$

$$\text{Electrode erosion rate, EWR} = \frac{W_{\text{BM}} - W_{\text{AM}}}{\text{MT}}\ (\text{gm/min}), \tag{2}$$

$$\text{Radial overcut, ROC (mm)} = \tan^{-1}\left\{\frac{\text{DT} - \text{DE}}{2}\right\}, \tag{3}$$

$$\text{Taper angle, } \theta\ (\text{deg}) = \tan^{-1}\left\{\frac{\text{DT} - \text{DB}}{2\text{t}}\right\}, \tag{4}$$

where W_{initial} and W_{final} are the weights of the workpiece before and after machining (g), W_{BM} and W_{AM} are the weights of the electrode before and after machining (g), MT is the time taken for machining (min), DT is the top diameter of drilled hole (mm), DB is the bottom diameter of drilled hole (mm), and DE is the diameter of electrode (mm).

The SR is measured using Mitutoyo (SURFTEST SJ-210) surface roughness tester. The geometrical tolerance results obtained from PC-DMIS metrology software are depicted in Figure 4 that is utilized to quantify the circularity and cylindricity for circular holes contrived in Si_3N_4–TiN workpiece.

3. Results and Discussions

3.1. Taguchi Methodology for Response Factors. In this investigation, negative polarity is selected as it increments the

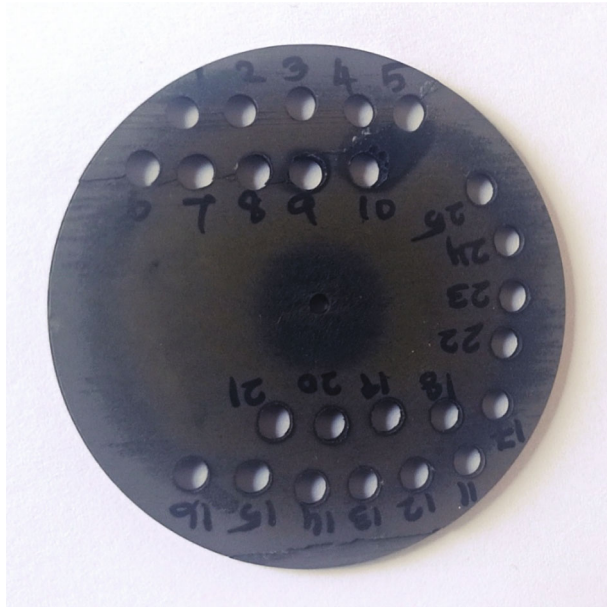

Figure 2: Machined Si_3N_4–TiN workpiece.

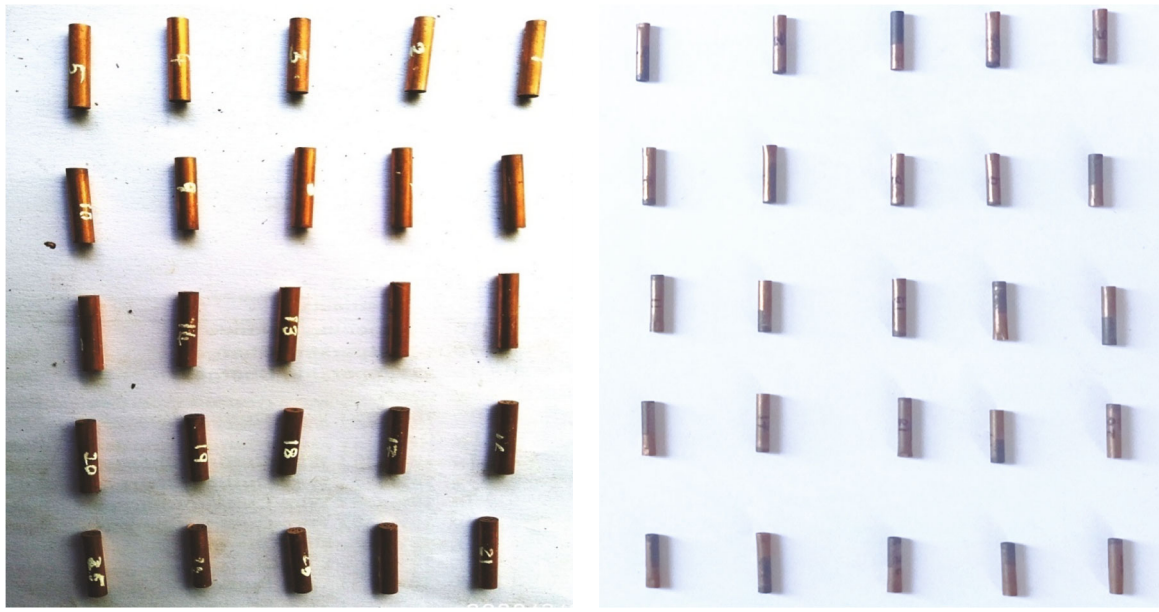

(a) (b)

Figure 3: Cylindrical shaped electrodes: (a) before machining; (b) after machining.

MRR and reduces the EWR by bombarding the electrode by electrons present in the discharge section and workpiece by positive ions [1]. The MRR increases as the PON and the pulse current increments. It is ascertained that the dielectric pressure and the POFF does not impact mostly on the output factor and also the SV has average output factor. To get increased material removal rate, the pulse current and the PON should be increased. The EWR has effects similar to that of MRR. In this scenario also, as the PON and the pulse current increments, the electrode erosion rate reduces. It is noticed that the dielectric pressure and the POFF does not impact much on the output factor and SV has average impact. To decrease the electrode erosion rate, moderate pulse-on time and pulse current are enforced. To achieve good surface, moderate pulse-on time and high gap voltage are enforced. From the main effect plot, it is evident that the surface quality decreases as the pulse current increments. The gap voltage increases the overall ROC, and the top radial would be reduced by employing lower discharge current and DP and higher SV. The θ could be reduced by decreasing pulse current and average DP. It is also observed that the low pulse current increases the taper angle

Table 1: Experimental input parameters.

Variables	Symbols	Units	Levels				
			1	2	3	4	5
Pulse current	I	amps	4	6	8	10	12
Pulse-on time	PON	μsec	5	6	7	8	9
Pulse-off time	POFF	μsec	2	4	6	8	10
Dielectric pressure	DP	kg/cm^2	12	14	16	18	20
Spark gap voltage	SV	Volts	28	30	32	34	36

drastically. To decrease the circularity, moderate discharge current and PON are employed, and the voltage should be maintained low. The effect of the DP and the POFF is high in circularity. The cylindricity is less at moderately high pulse current, and the main effect plot proves that decreasing pulse current increments the cylindricity profoundly. On the other hand, the lower PON increases the cylindricity, and SV should be continued low.

3.2. GRA Optimization. Grey relational analysis transforms the single-objective condition into an individual response optimization [1]. The GRA proceeds through the accompanying advances.

Step 1. Normalization is done for all the experimental output parameters by the successive equations.

Normalization for higher-the-better,

$$x_i(k) = \frac{g_i(k) - \min g_i(k)}{\max g_i(k) - \min g_i(k)}. \quad (5)$$

Normalization for lower-the-better,

$$x_i(k) = \frac{\max g_i(k) - g_i(k)}{\max g_i(k) - \min g_i(k)}, \quad (6)$$

where $x_i(k)$ is normalized value for obtained response, min $g_i(k)$ is the least value of $g_i(k)$ for kth response, max $g_i(k)$ is the highest value of $g_i(k)$ for kth response, "i" is the experimental number, and "k" is the comparability sequence.

Step 2. Grey relational coefficient delineates the correlation among the desired and actual normalized experimental response. The GRC value is determined as follows:

$$\varphi_i(k) = \frac{\Delta_{\min} + \varphi\Delta_{\max}}{\Delta_{oi}(k) + \varphi\Delta_{\max}}, \quad (7)$$

where $\Delta(k)$ is a deviation sequence, i.e., $\Delta_{oi}(k) = |g_i(k) - x_i(k)|$; φ is a unique coefficient which sustains between 0 and 1 (usually assumed as $\varphi = 0.5$); k is a GRC; $\Delta_{\min}$ (least deviation sequence) is the lowest value of $\Delta(k)$; and $\Delta_{\max}$ (highest deviation sequence) is the highest value of $\Delta_{oi}(k)$.

Table 2: Table design and time taken for machining.

Run	Input machining factors					Machining time (t) in min
	I	PON	POFF	DP	SV	
1	4	5	2	12	28	29.09
2	4	6	4	14	30	27.33
3	4	7	6	16	32	24.45
4	4	8	8	18	34	21.36
5	4	9	10	20	36	19.53
6	6	5	4	16	34	30.29
7	6	6	6	18	36	28.04
8	6	7	8	20	28	26.25
9	6	8	10	12	30	23.47
10	6	9	2	14	32	20.25
11	8	5	6	20	30	32.25
12	8	6	8	12	32	30.12
13	8	7	10	14	34	25.43
14	8	8	2	16	36	23.45
15	8	9	4	18	28	19.23
16	10	5	8	14	36	28.29
17	10	6	10	16	28	26.32
18	10	7	2	18	30	24.11
19	10	8	4	20	32	21.35
20	10	9	6	12	34	18.25
21	12	5	10	18	32	31.23
22	12	6	2	20	34	27.25
23	12	7	4	12	36	23.45
24	12	8	6	14	28	19.58
25	12	9	8	16	30	17.45

Step 3. The grey relational grade is obtained from average value of GRC. The GRG is calculated as follows:

$$\theta_i = \frac{1}{n}\sum_{i=1}^{n} \varphi_i(k), \quad (8)$$

where θ_i is the GRG of ith trial, n is a number of trials, and $\varphi_i(k)$ is a GRC.

Table 3: Experimental results for responses after EDM.

Run	MRR (g/min)	EWR (g/min)	SR (μm)	ROC (mm)	θ (deg)	CIR (mm)	CYL (mm)
1	0.00298	0.00098	1.44	0.30	0.0488	0.0744	0.1282
2	0.00240	0.00032	0.71	0.24	0.0810	0.0491	0.0299
3	0.00172	0.00053	2.53	0.23	0.0985	0.0436	0.0545
4	0.00444	0.00111	0.56	0.18	0.0848	0.0525	0.0685
5	0.00220	0.00058	4.80	0.15	0.3140	0.0260	0.0272
6	0.00139	0.00065	0.87	0.38	0.0612	0.1752	0.1549
7	0.00280	0.00073	1.51	0.15	0.5622	0.0190	0.0094
8	0.00275	0.00083	2.87	0.19	0.3540	0.0376	0.0392
9	0.00409	0.00080	1.69	0.20	0.3667	0.0441	0.0748
10	0.00192	0.00069	0.92	0.16	0.0550	0.1465	0.0520
11	0.00198	0.00085	1.38	0.19	0.1229	0.0429	0.0763
12	0.00256	0.00079	3.99	0.20	0.0611	0.0320	0.0496
13	0.00204	0.00040	3.83	0.17	0.5150	0.1121	0.0973
14	0.00281	0.00116	1.27	0.21	0.0268	0.0509	0.0313
15	0.00312	0.00145	0.69	0.23	0.0893	0.0573	0.0818
16	0.00199	0.00059	3.26	0.20	0.0761	0.0205	0.0203
17	0.00151	0.00062	2.60	0.20	0.0871	0.0183	0.0320
18	0.00255	0.00123	1.15	0.12	0.0877	0.0303	0.0410
19	0.00207	0.00073	1.17	0.18	0.0951	0.0168	0.0277
20	0.00183	0.00029	2.52	0.19	0.0210	0.0473	0.0230
21	0.00117	0.00060	0.93	0.21	0.0244	0.0778	0.0307
22	0.00093	0.00079	0.65	0.06	0.0486	0.0557	0.0313
23	0.00219	0.00058	0.77	0.15	0.1098	0.0309	0.0120
24	0.00267	0.00040	1.42	0.24	0.2073	0.0137	0.0231
25	0.00186	0.00037	3.44	0.19	0.0355	0.0111	0.0216

In GRA, the GRG which is highest was given top ranking, and lower GRG is given last rank [1]. The calculated GRG for 25 experimental run orders is shown in Table 4. Figure 5 outlines the GRG for 25 experimental run orders, and Table 4 portrays the impact of input factor on the GRG. From Tables 4 and 5, it is evident that $A_5B_3C_2D_1E_5$ are the optimal input factor levels. Consequently, the 23rd experimental run order is the optimized group of input factors for best output response.

3.3. TOPSIS Optimization. Technique for order of preference by similarity to ideal solution is an ordinary MCDM optimization methodology that assists with selecting the better input factors among the enormous number of options which is having the shortest point from positive ideal solution and the largest point from negative ideal solution [1]. The MCDM using the TOPSIS methodology proceeds through the accompanying advances.

Step 1. First, all the information gathered from experimental run was utilized for developing decision matrix which comprises of n number of response factors which are complexions and m number of experimental runs that are the substitute result.

$$D_m = \begin{bmatrix} a_{11} & a_{12} & a_{13} & \cdots & \cdots & a_{1n} \\ a_{21} & a_{22} & a_{23} & \cdots & \cdots & a_{2n} \\ \vdots & \vdots & \vdots & \vdots & \vdots & \vdots \\ a_{m1} & a_{m2} & a_{m3} & \cdots & \cdots & a_{mn} \end{bmatrix}, \quad (9)$$

where a_{ij} is the measure of jth attribute to ith alternative.

Step 2. The accompanying condition gives the result for normalization of decision matrix.

$$\gamma_{ij} = \frac{a_{ij}}{\sqrt{\sum_{i=1}^{m} a_{ij}^2}}, \quad (10)$$

where γ_{ij} is normalized solution for $i = 1,2,3, \cdots, m$ and $j = 1,2,3, \cdots, n$.

Step 3. The weights of every characteristic are fixed, and for the whole attributes, the total sum of weightage should be

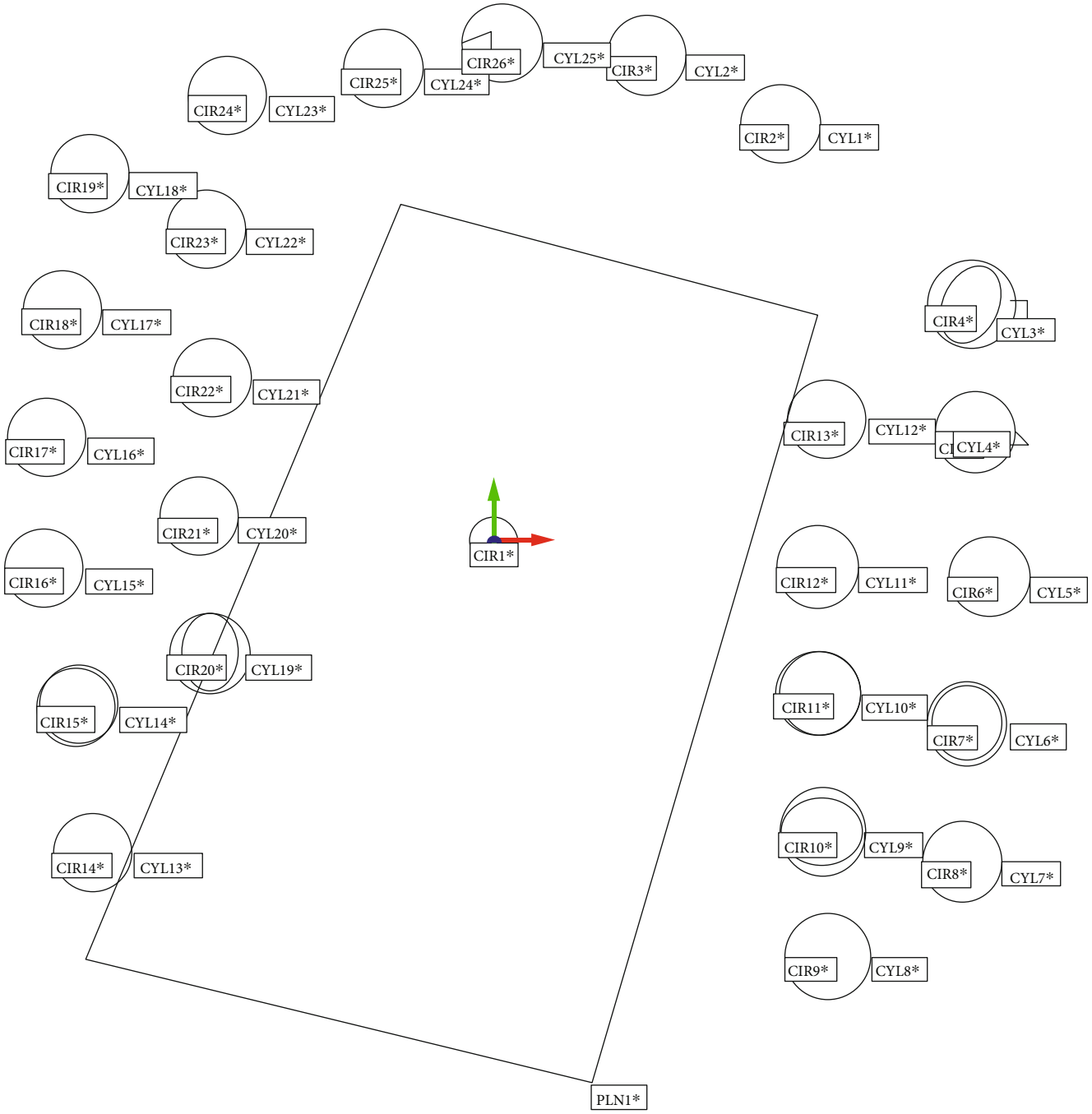

Figure 4: Circularity and cylindricity measurement.

equivalent to 1. By utilizing the accompanying condition, the weighted normalized decision matrix is determined.

$$\varphi_{ij} = w_j \gamma_{ij}, \tag{11}$$

where $\sum_{j=1}^{n} w_j = 1$.

Step 4. The positive ideal solution (PIS) and negative ideal solution (NIS) can be determined by

$$\begin{aligned} \varphi^{+} &= (\varphi_1^{+}, \varphi_2^{+}, \cdots \varphi_n^{+}) \\ &= \left\{ \left(\max \varphi_{ij} | j \in J_1 \right), \left(\min \varphi_{ij} | j \in J_2, i = 1, 2, \cdots n \right) \right\}, \end{aligned} \tag{12}$$

Table 4: Grey relational analysis.

Run	Normalization							Grey relational coefficient								
	MRR (g/min)	EWR (g/min)	SR (μm)	ROC (mm)	θ (deg)	CIR (mm)	CYL (mm)	MRR (g/min)	EWR (g/min)	SR (μm)	ROC (mm)	θ (deg)	CIR (mm)	CYL (mm)	GRG	Rank
1	0.10021	0.99889	0.70737	0.24714	0.94867	0.61426	0.90125	0.35720	0.99778	0.63081	0.39909	0.90689	0.56450	0.83507	0.67019	15
2	0.07176	0.99973	0.86105	0.43250	0.88917	0.76843	0.85911	0.35008	0.99945	0.78254	0.46838	0.81856	0.68347	0.78016	0.69752	10
3	0.03847	0.99946	0.47789	0.46339	0.85683	0.80195	0.69003	0.34211	0.99892	0.48919	0.48234	0.77740	0.71628	0.61731	0.63194	22
4	0.17148	0.99872	0.89263	0.61786	0.88215	0.74771	0.59381	0.37636	0.99745	0.82322	0.56680	0.80925	0.66464	0.55176	0.68421	14
5	0.06174	0.99939	0	0.71053	0.45863	0.90920	0.87766	0.34764	0.99879	0.33333	0.63334	0.48014	0.84631	0.80342	0.63471	21
6	1	0.99930	0.82737	0	0.92575	0	0	1	0.99861	0.74335	0.33333	0.87071	0.33333	0.33333	0.65895	16
7	0.09131	0.99921	0.69263	0.71053	0	0.95186	1	0.35494	0.99842	0.61930	0.63334	0.33333	0.91217	1	0.69307	12
8	0.08887	0.99908	0.40632	0.58696	0.38471	0.83851	0.79519	0.35433	0.99817	0.45717	0.54762	0.44832	0.75587	0.70941	0.61013	23
9	0.15437	0.99911	0.65474	0.55607	0.36125	0.79890	0.55052	0.37157	0.99823	0.59153	0.52970	0.43908	0.71317	0.52660	0.59570	24
10	0.04830	0.99926	0.81684	0.67964	0.93716	0.17489	0.70722	0.34442	0.99853	0.73190	0.60949	0.88835	0.37733	0.63069	0.65439	17
11	0.05123	0.99906	0.72000	0.58696	0.81174	0.80622	0.54021	0.34512	0.99811	0.64103	0.54762	0.72647	0.72069	0.52095	0.64286	20
12	0.07948	0.99913	0.17053	0.55607	0.92594	0.87264	0.72371	0.35198	0.99826	0.37609	0.52970	0.87099	0.79699	0.64409	0.65259	18
13	0.05436	1	0.20421	0.64875	0.08722	0.38452	0.39588	0.34587	1	0.38587	0.58737	0.35391	0.44824	0.45285	0.51059	25
14	0.09180	0.99866	0.74316	0.52518	0.98926	0.75746	0.84948	0.35506	0.99732	0.66064	0.51291	0.97898	0.67337	0.76862	0.70670	6
15	0.10696	0.99829	0.86526	0.46339	0.87383	0.71846	0.50241	0.35893	0.99660	0.78773	0.48234	0.79851	0.63977	0.50121	0.65215	19
16	0.05182	0.99938	0.32421	0.55607	0.89822	0.94272	0.92509	0.34526	0.99875	0.42525	0.52970	0.83087	0.89721	0.86970	0.69953	8
17	0.02826	0.99935	0.46316	0.55607	0.87795	0.95612	0.84467	0.33973	0.99870	0.48223	0.52970	0.80380	0.91933	0.76298	0.69092	13
18	0.07909	0.99857	0.76842	0.80321	0.87679	0.88300	0.78282	0.35189	0.99715	0.68345	0.71758	0.80229	0.81037	0.69717	0.72284	4
19	0.05578	0.99920	0.76421	0.61786	0.86321	0.96527	0.87423	0.34621	0.99840	0.67954	0.56680	0.78518	0.93504	0.79901	0.73003	2
20	0.04390	0.99976	0.48000	0.58696	1	0.77940	0.90653	0.34338	0.99951	0.49020	0.54762	1	0.69387	0.84250	0.70244	7
21	0.01164	0.99937	0.81474	0.52518	0.99375	0.59354	0.85361	0.33594	0.99875	0.72965	0.51291	0.98766	0.55160	0.77352	0.69858	9
22	0	0	1	1	0.94904	0.72821	0.84948	0.33333	0.33333	1	1	0.90750	0.64785	0.76862	0.71295	5
23	**0.06150**	**0.99940**	**0.84842**	**0.71053**	**0.83595**	**0.87934**	**0.98213**	**0.34758**	**0.99880**	**0.76737**	**0.63334**	**0.75296**	**0.80560**	**0.96549**	**0.75302**	**1**
24	0.08476	0.99963	0.71158	0.43250	0.65579	0.98416	0.90584	0.35330	0.99926	0.63418	0.46838	0.59227	0.96929	0.84153	0.69403	11
25	0.04537	0.99966	0.28632	0.58696	0.97324	1	0.91615	0.34373	0.99932	0.41197	0.54762	0.94921	1	0.85639	0.72975	3

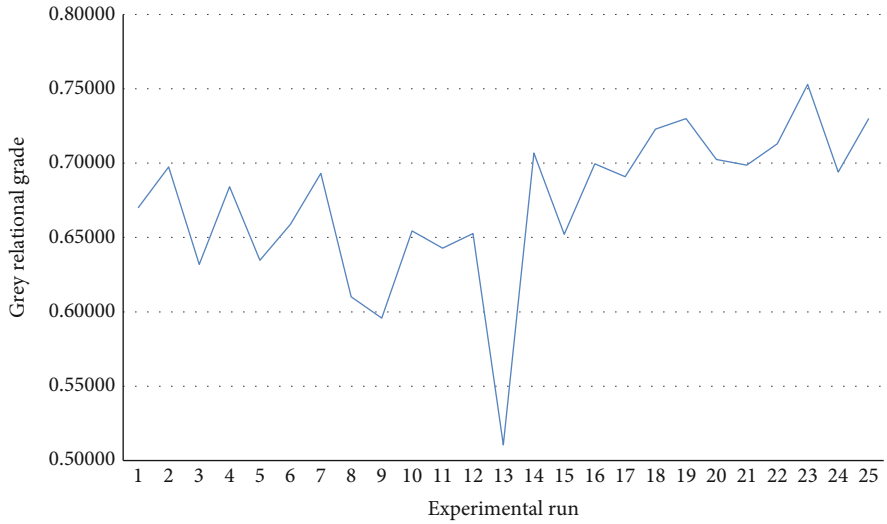

Figure 5: GRG for experimental run.

Table 5: Factor effect on GRG.

Parameter	Grey relational grade					Optimal level	Difference	Rank
	1	2	3	4	5			
I	0.66371	0.64245	0.63298	0.70915	**0.71766**	5	0.08469	1
PON	0.67402	0.68213	**0.68941**	0.64122	0.67469	3	0.04819	2
POFF	0.69341	**0.69833**	0.69287	0.67524	0.66610	2	0.03224	4
DP	**0.69017**	0.66121	0.67479	0.68365	0.66613	1	0.02896	5
SV	0.66349	0.67773	0.67350	0.65383	**0.69741**	5	0.03392	3

$$\varphi^{-} = (\varphi_1^{-}, \varphi_2^{-}, \cdots . \varphi_n^{-}) = \left\{ \left(\min \varphi_{ij} | j \in J_1 \right), \left(\max \varphi_{ij} | j \in J_2, i = 1, 2, \cdots n \right) \right\}, \tag{13}$$

where J_1 and J_2 are sets of beneficial attribute and nonbeneficial attribute, respectively.

Step 5. Separation proportions of the entire options are determined from PIS and NIS

$$S_i^{+} = \sqrt{\sum_{j=1}^{n} \left(\varphi_{ij} - \varphi_i^{+} \right)^2}, \tag{14}$$

$$S_i^{-} = \sqrt{\sum_{j=1}^{n} \left(\varphi_{ij} - \varphi_i^{-} \right)^2}, \tag{15}$$

where $i = 1,2,3, \cdots, m$.

Step 6. The relative similarity index (SI) of every parameter is determined utilizing the accompanying equation

$$\mathrm{SI} = \frac{S_i^{-}}{S_i^{+} - S_i^{-}}. \tag{16}$$

In TOPSIS, the first part is to change the outcomes to a decision matrix comprising of output responses (attributes) in columns and exploratory trials (alternatives) in rows as delineated in Equation (9). By utilizing Equation (10), the decision matrix is normalized, and relative weightage is doled to all entities. Then, equivalent relative weightage is fixed to entire seven responses, viz., material removal rate, electrode wear rate, surface roughness, radial overcut, taper angle, circularity, and cylindricity. The weighted normalization numbers were determined by using Equation (11). Using Equations (12) and (13), the positive ideal solution and negative ideal solution are obtained from the normalization matrix. Equations (14) and (15) are utilized to ascertain the separation measures of every alternative from PIS and NIS. Likewise, Equation (16) is employed to ascertain the similarity index for all the options by finding the separation measures [1].

Based on the TOPSIS optimization, the normalized matrix, weighted-normalized matrix, separation evaluated

Table 6: TOPSIS.

Run	Normalization							Weighted normalized matrix							Separation			
	MRR (g/min)	EWR (g/min)	SR (μm)	ROC (mm)	θ (deg)	CIR (mm)	CYL (mm)	MRR (g/min)	EWR (g/min)	SR (μm)	ROC (mm)	θ (deg)	CIR (mm)	CYL (mm)	S^+	S^-	SI	Rank
1	0.13596	0.28222	0.05264	0.16713	0.08112	0.14294	0.19924	0.01944	0.04036	0.00753	0.02390	0.01160	0.02044	0.02849	0.55500	4.84144	0.89715	23
2	0.12524	0.20437	0.15886	0.18570	0.35077	0.12007	0.21757	0.01791	0.02922	0.02272	0.02655	0.05016	0.01717	0.03111	0.53983	4.82192	0.89932	9
3	0.08427	0.23694	0.07426	0.04642	0.05385	0.13232	0.16201	0.01205	0.03388	0.01062	0.00664	0.00770	0.01892	0.02317	0.55256	4.84025	0.89754	21
4	0.08604	0.29544	0.11938	0.19498	0.02566	0.13858	0.09104	0.01230	0.04225	0.01707	0.02788	0.00367	0.01982	0.01302	0.54541	4.83305	0.89859	14
5	0.05879	0.17421	0.08648	0.14856	0.05264	0.39886	0.15125	0.00841	0.02491	0.01237	0.02124	0.00753	0.05704	0.02163	0.55111	4.83633	0.89770	20
6	0.06348	0.18665	0.10998	0.16713	0.09092	0.04574	0.08057	0.00908	0.02669	0.01573	0.02390	0.01300	0.00654	0.01152	0.54580	4.83398	0.89855	15
7	0.06063	0.21561	0.12972	0.17641	0.11756	0.11680	0.22193	0.00867	0.03083	0.01855	0.02523	0.01681	0.01670	0.03174	0.54352	4.82978	0.89885	11
8	0.09554	0.36867	0.06486	0.21355	0.08542	0.15601	0.23793	0.01366	0.05272	0.00927	0.03054	0.01222	0.02231	0.03402	0.55431	4.83905	0.89722	22
9	0.07349	0.08088	0.06674	0.22283	0.07748	0.13368	0.08697	0.01051	0.01157	0.00954	0.03187	0.01108	0.01912	0.01244	0.55111	4.83924	0.89776	19
10	0.09131	0.24891	0.13536	0.27854	0.04668	0.20256	0.37289	0.01306	0.03559	0.01936	0.03983	0.00668	0.02897	0.05332	0.54415	4.82824	0.89871	12
11	0.06706	0.14619	0.07238	0.13927	0.10503	0.08413	0.03490	0.00959	0.02091	0.01035	0.01992	0.01502	0.01203	0.00499	0.55104	4.83936	0.89777	18
12	0.07808	0.31273	0.10810	0.11142	0.08389	0.08249	0.11925	0.01117	0.04472	0.01546	0.01593	0.01200	0.01180	0.01705	0.54765	4.83475	0.89825	16
13	0.65497	0.16592	0.08178	0.35282	0.05854	0.47700	0.45055	0.09366	0.02373	0.01169	0.05045	0.00837	0.06821	0.06443	0.55909	4.83445	0.89633	25
14	0.08421	0.20976	0.26978	0.17641	0.33862	0.10237	0.11402	0.01204	0.03000	0.03858	0.02523	0.04842	0.01464	0.01630	0.52371	4.80696	0.90175	5
15	0.03583	0.15179	0.08742	0.19498	0.02334	0.21182	0.08930	0.00512	0.02171	0.01250	0.02788	0.00334	0.03029	0.01277	0.54916	4.83716	0.89805	17
16	0.05604	0.07462	0.23688	0.17641	0.02011	0.12878	0.06690	0.00801	0.01067	0.03387	0.02523	0.00288	0.01842	0.00957	0.52732	4.81669	0.90133	7
17	0.08574	0.18449	0.14194	0.13927	0.53778	0.05173	0.02734	0.01226	0.02638	0.02030	0.01992	0.07690	0.00740	0.00391	0.54420	4.82311	0.89861	13
18	0.06259	0.02588	0.36002	0.15784	0.49263	0.30520	0.28301	0.00895	0.00370	0.05148	0.02257	0.07045	0.04364	0.04047	0.51363	4.79046	0.90316	3
19	0.07833	0.20058	0.37506	0.18570	0.05845	0.08712	0.14427	0.01120	0.02868	0.05363	0.02655	0.00836	0.01246	0.02063	0.50810	4.79635	0.90421	2
20	0.04624	0.15649	0.24440	0.18570	0.08329	0.04982	0.09308	0.00661	0.02238	0.03495	0.02655	0.01191	0.00712	0.01331	0.52639	4.81479	0.90145	6
21	0.05264	0.13404	0.23782	0.21355	0.09422	0.11871	0.15852	0.00753	0.01917	0.03401	0.03054	0.01347	0.01697	0.02267	0.52711	4.81464	0.90132	8
22	0.06100	0.15108	0.30644	0.18570	0.07279	0.05581	0.05905	0.00872	0.02160	0.04382	0.02655	0.01041	0.00798	0.00844	0.51746	4.80630	0.90280	4
23	**0.06721**	**0.14790**	**0.45120**	**0.13927**	**0.30036**	**0.07079**	**0.07912**	**0.00961**	**0.02115**	**0.06452**	**0.01992**	**0.04295**	**0.01012**	**0.01131**	**0.49748**	**4.78251**	**0.90578**	**1**
24	0.08163	0.10071	0.13348	0.22283	0.19829	0.03730	0.06719	0.01167	0.01440	0.01909	0.03187	0.02836	0.00533	0.00961	0.54161	4.82841	0.89914	10
25	0.65497	0.16592	0.08178	0.35282	0.05854	0.47700	0.45055	0.09366	0.02373	0.01169	0.05045	0.00837	0.06821	0.06443	0.55909	4.83445	0.89634	24

Table 7: Mean similarity index of each parameter at entry level.

Parameter	Similarity index					Optimal level	Difference	Rank
	1	2	3	4	5			
I	0.89806	0.89722	0.89843	0.90108	**0.90175**	5	0.00453	1
PON	0.89922	0.89657	**0.90029**	0.90001	0.89845	3	0.00373	2
POFF	0.90072	**0.90118**	0.89895	0.89835	0.89835	2	0.00283	4
DP	**0.90008**	0.89897	0.89856	0.89999	0.89994	1	0.00111	5
SV	0.89803	0.89787	0.90001	0.89955	**0.90108**	5	0.00321	3

Table 8: Initial random population.

Run	Input parameter					Response							GRG	Rank
	I	PON	POFF	DP	SV	MRR	EWR	SR	ROC	θ	CIR	CYL		
1	4	5	2	12	28	0.00298	0.00098	1.44	0.30	0.0488	0.0744	0.1282	0.67019	15
2	4	6	4	14	30	0.00240	0.00032	0.71	0.24	0.0810	0.0491	0.0299	0.69752	10
3	4	7	6	16	32	0.00172	0.00053	2.53	0.23	0.0985	0.0436	0.0545	0.63194	22
4	4	8	8	18	34	0.00444	0.00111	0.56	0.18	0.0848	0.0525	0.0685	0.68421	14
5	4	9	10	20	36	0.00220	0.00058	4.80	0.15	0.3140	0.0260	0.0272	0.63471	21
6	6	5	4	16	34	0.02139	0.00065	0.87	0.38	0.0612	0.1752	0.1549	0.65895	16
7	6	6	6	18	36	0.00280	0.00073	1.51	0.15	0.5622	0.0190	0.0094	0.69307	12
8	6	7	8	20	28	0.00275	0.00083	2.87	0.19	0.3540	0.0376	0.0392	0.61013	23
9	6	8	10	12	30	0.00409	0.00080	1.69	0.20	0.3667	0.0441	0.0748	0.59570	24
10	6	9	2	14	32	0.00192	0.00069	0.92	0.16	0.0550	0.1465	0.0520	0.65439	17
11	8	5	6	20	30	0.00198	0.00085	1.38	0.19	0.1229	0.0429	0.0763	0.64286	20
12	8	6	8	12	32	0.00256	0.00079	3.99	0.20	0.0611	0.0320	0.0496	0.65259	18
13	8	7	10	14	34	0.00204	0.00010	3.83	0.17	0.5150	0.1121	0.0973	0.51059	25
14	8	8	2	16	36	0.00281	0.00116	1.27	0.21	0.0268	0.0509	0.0313	0.70670	6
15	8	9	4	18	28	0.00312	0.00145	0.69	0.23	0.0893	0.0573	0.0818	0.65215	19
16	10	5	8	14	36	0.00199	0.00059	3.26	0.20	0.0761	0.0205	0.0203	0.69953	8
17	10	6	10	16	28	0.00151	0.00062	2.60	0.20	0.0871	0.0183	0.0320	0.69092	13
18	10	7	2	18	30	0.00255	0.00123	1.15	0.12	0.0877	0.0303	0.0410	0.72284	4
19	10	8	4	20	32	0.00207	0.00073	1.17	0.18	0.0951	0.0168	0.0277	0.73003	2
20	10	9	6	12	34	0.00183	0.00029	2.52	0.19	0.0210	0.0473	0.0230	0.70244	7
21	12	5	10	18	32	0.00117	0.00060	0.93	0.21	0.0244	0.0778	0.0307	0.69858	9
22	12	6	2	20	34	0.00093	0.79000	0.05	0.06	0.0486	0.0557	0.0313	0.71295	5
23	**12**	**7**	**4**	**12**	**36**	**0.00219**	**0.00058**	**0.77**	**0.15**	**0.1098**	**0.0309**	**0.0120**	**0.75302**	**1**
24	12	8	6	14	28	0.00267	0.00040	1.42	0.24	0.2073	0.0137	0.0231	0.69403	11
25	12	9	8	16	30	0.00186	0.00037	3.44	0.19	0.0355	0.0111	0.0216	0.72975	3
Mean	8	7	6	16	32									

data, and SI of every option are delineated in Table 6. The alternative result with highest SI value is the predominant, and the trails are ranked depending upon the SI. The 23rd experimental run is the good run, and the 13th is the poor among every one of the other options. Table 7 displays the determined mean similarity index of all the input factors at all the levels.

3.4. TLBO Algorithms. TLBO algorithms depict the teaching, and learning phenomenon takes place in the classroom [1]. The current work was centered on maximization of material removal rate and minimization of electrode erosion rate, SR, ROC, θ, circularity, and cylindricity, respectively. The regression equation for maximization and minimization of output factors is delineated in Equation (17) to Equation (23). Additionally, the parametric bounds are delineated in Equation (24) to Equation (28).

Maximization:

$$\text{MRR} = 0.00047 + 0.000367\,I + 0.000214\,\text{PON} - 0.000039\,\text{POFF} - 0.000050\,\text{DP} - 0.000025\,\text{SV}. \quad (17)$$

Table 9: Teacher phase–updated process parameter and responses.

S. no	New input parameter					Bounded input parameter					New response							GRG	Rank
	I	PON	POFF	DP	SV	I	PON	POFF	DP	SV	MRR	EWR	SR	ROC	θ	CIR	CYL		
1	2.2	3.9	-0.6	9	24.6	4	3.9	2	12	28	0.00666	0.01322	0.56	0.31	0.0450	0.0950	0.1165	0.60515	23
2	2.2	5.45	2.7	12.5	28.3	4	5.45	2.7	12.5	28.3	0.00559	0.03850	0.93	0.29	0.0750	0.0858	0.1034	0.69752	10
3	2.2	7	6	16	32	4	7	6	16	32	0.00445	0.03060	2.02	0.22	0.2027	0.0672	0.0720	0.63194	21
4	2.2	8.55	9.3	19.5	35.7	4	8.55	9.3	19.5	35.7	0.00332	0.02270	3.12	0.16	0.3304	0.0486	0.0406	0.68421	14
5	2.2	10.1	12.6	23	39.4	4	9	10	20	36	0.00294	0.03060	3.35	0.15	0.3537	0.0439	0.0349	0.63471	20
6	5.1	3.9	2.7	16	35.7	5.1	3.9	2.7	16	35.7	0.00720	0.11713	0.84	0.23	0.1171	0.0921	0.0814	0.65895	15
7	5.1	5.45	6	19.5	39.4	5.1	5.45	6	19.5	36	0.00554	0.09817	1.78	0.19	0.2230	0.0682	0.0594	0.69307	12
8	5.1	7	9.3	23	24.6	5.1	7	9.3	20	28	0.00270	0.03376	2.49	0.21	0.2586	0.0373	0.0654	0.61013	22
9	5.1	8.55	12.6	9	28.3	5.1	8.55	10	9	28.3	0.00213	0.24074	3.51	0.27	0.2231	0.0516	0.0710	0.59570	24
10	5.1	10.1	-0.6	12.5	32	5.1	9	2	12.5	32	0.00371	0.03692	1.31	0.22	0.0887	0.0753	0.0641	0.65439	16
11	8	3.9	6	23	28.3	8	3.9	6	20	28.3	0.00432	0.11555	1.08	0.23	0.1253	0.0497	0.0740	0.64286	19
12	8	5.45	9.3	9	32	8	5.45	9.3	12	32	0.00370	0.05825	2.81	0.24	0.1874	0.0545	0.0614	0.65259	17
13	8	7	12.6	12.5	35.7	8	7	10	12.5	35.7	0.00316	0.05667	3.35	0.20	0.2392	0.0507	0.0388	0.51059	25
14	8	8.55	-0.6	16	39.4	8	8.55	2	16	36	0.00351	0.10291	1.12	0.16	0.0898	0.0646	0.0339	0.70670	6
15	8	10.1	2.7	19.5	24.6	8	9	2.7	19.5	28	0.00170	0.07684	0.81	0.18	0.0771	0.0407	0.0463	0.65215	18
16	10.9	3.9	9.3	12.5	39.4	10.9	3.9	9.3	12.5	36	0.00432	0.05156	2.66	0.21	0.1647	0.0543	0.0435	0.69953	8
17	10.9	5.45	12.6	16	24.6	10.9	5.45	10	16	28	0.00182	0.00811	2.48	0.21	0.1587	0.0260	0.0485	0.69092	13
18	10.9	7	-0.6	19.5	28.3	10.9	7	2	19.5	28.3	0.00217	0.16769	0.26	0.18	0.0092	0.0399	0.0436	0.72284	4
19	10.9	8.55	2.7	23	32	10.9	8.55	2.7	20	32	0.00163	0.16927	0.79	0.13	0.0610	0.0361	0.0211	0.73003	2
20	10.9	10.1	6	9	35.7	10.9	9	6	9	35.7	0.00183	0.03455	2.56	0.18	0.0993	0.0515	0.0207	0.70244	7
21	13.8	3.9	12.6	19.5	32	12	3.9	10	19.5	32	0.00290	0.13688	2.24	0.18	0.1789	0.0270	0.0359	0.69858	9
22	13.8	5.45	-0.6	23	35.7	12	5.45	2	20	35.7	0.00392	0.27592	0.34	0.14	0.0341	0.0523	0.0265	0.71295	5
23	**13.8**	**7**	**2.7**	**9**	**39.4**	**12**	**7**	**2.7**	**9**	**36**	**0.00335**	**0.06894**	**1.36**	**0.19**	**0.0014**	**0.0667**	**0.0321**	**0.75302**	**1**
24	13.8	8.55	6	12.5	24.6	12	8.55	6	12.5	28	0.00038	0.01559	1.91	0.20	0.0514	0.0297	0.0332	0.69403	11
25	13.8	10.1	9.3	16	28.3	12	9	9.3	16	28.3	0.00060	0.01717	2.70	0.17	0.1506	0.0101	0.0186	0.72975	3

Table 10: Combined population.

Run	Combined input parameter					New response							GRG	Rank
	I	PON	POFF	DP	SV	MRR	EWR	SR	ROC	θ	CIR	CYL		
1	4	5	2	12	28	0.00298	0.00098	1.44	0.30	0.0488	0.0744	0.1282	0.67019	49
2	4	6	4	14	30	0.00240	0.00032	0.71	0.24	0.0810	0.0491	0.0299	0.69752	21
3	4	7	6	16	32	0.00172	0.00053	2.53	0.23	0.0985	0.0436	0.0545	0.63194	46
4	4	8	8	18	34	0.00444	0.00111	0.56	0.18	0.0848	0.0525	0.0685	0.68421	23
5	4	9	10	20	36	0.00220	0.00058	4.80	0.15	0.3140	0.0260	0.0272	0.63471	38
6	6	5	4	16	34	0.02139	0.00065	0.87	0.38	0.0612	0.1752	0.1549	0.65895	19
7	6	6	6	18	36	0.00280	0.00073	1.51	0.15	0.5622	0.0190	0.0094	0.69307	6
8	6	7	8	20	28	0.00275	0.00083	2.87	0.19	0.3540	0.0376	0.0392	0.61013	40
9	6	8	10	12	30	0.00409	0.00080	1.69	0.20	0.3667	0.0441	0.0748	0.59570	44
10	6	9	2	14	32	0.00192	0.00069	0.92	0.16	0.0550	0.1465	0.0520	0.65439	24
11	8	5	6	20	30	0.00198	0.00085	1.38	0.19	0.1229	0.0429	0.0763	0.64286	41
12	8	6	8	12	32	0.00256	0.00079	3.99	0.20	0.0611	0.0320	0.0496	0.65259	47
13	8	7	10	14	34	0.00204	0.00010	3.83	0.17	0.5150	0.1121	0.0973	0.51059	48
14	8	8	2	16	36	0.00281	0.00116	1.27	0.21	0.0268	0.0509	0.0313	0.70670	27
15	8	9	4	18	28	0.00312	0.00145	0.69	0.23	0.0893	0.0573	0.0818	0.65215	37
16	10	5	8	14	36	0.00199	0.00059	3.26	0.20	0.0761	0.0205	0.0203	0.69953	34
17	10	6	10	16	28	0.00151	0.00062	2.60	0.20	0.0871	0.0183	0.0320	0.69092	39
18	10	7	2	18	30	0.00255	0.00123	1.15	0.12	0.0877	0.0303	0.0410	0.72284	16
19	10	8	4	20	32	0.00207	0.00073	1.17	0.18	0.0951	0.0168	0.0277	0.73003	20
20	10	9	6	12	34	0.00183	0.00029	2.52	0.19	0.0210	0.0473	0.0230	0.70244	31
21	12	5	10	18	32	0.00117	0.00060	0.93	0.21	0.0244	0.0778	0.0307	0.69858	22
22	12	6	2	20	34	0.00093	0.79000	0.05	0.06	0.0486	0.0557	0.0313	0.71295	17
23	12	7	4	12	36	0.00219	0.00058	0.77	0.15	0.1098	0.0309	0.0120	0.75302	2
24	12	8	6	14	28	0.00267	0.00040	1.42	0.24	0.2073	0.0137	0.0231	0.69403	25
25	12	9	8	16	30	0.00186	0.00037	3.44	0.19	0.0355	0.0111	0.0216	0.72975	36
26	4	3.9	2	12	28	0.00666	0.01322	0.56	0.31	0.0450	0.0950	0.1165	0.60515	43
27	4	5.45	2.7	12.5	28.3	0.00559	0.03850	0.93	0.29	0.0750	0.0858	0.1034	0.69752	12
28	4	7	6	16	32	0.00445	0.03060	2.02	0.22	0.2027	0.0672	0.0720	0.63194	35
29	4	8.55	9.3	19.5	35.7	0.00332	0.02270	3.12	0.16	0.3304	0.0486	0.0406	0.68421	18
30	4	9	10	20	36	0.00294	0.03060	3.35	0.15	0.3537	0.0439	0.0349	0.63471	33
31	5.1	3.9	2.7	16	35.7	0.00720	0.11713	0.84	0.23	0.1171	0.0921	0.0814	0.65895	26
32	5.1	5.45	6	19.5	36	0.00554	0.09817	1.78	0.19	0.2230	0.0682	0.0594	0.69307	14
33	5.1	7	9.3	20	28	0.00270	0.03376	2.49	0.21	0.2586	0.0373	0.0654	0.61013	42
34	5.1	8.55	10	9	28.3	0.00213	0.24074	3.51	0.27	0.2231	0.0516	0.0710	0.59570	45
35	5.1	9	2	12.5	32	0.00371	0.03692	1.31	0.22	0.0887	0.0753	0.0641	0.65439	28
36	8	3.9	6	20	28.3	0.00432	0.11555	1.08	0.23	0.1253	0.0497	0.0740	0.64286	32
37	8	5.45	9.3	12	32	0.00370	0.05825	2.81	0.24	0.1874	0.0545	0.0614	0.65259	29
38	8	7	10	12.5	35.7	0.00316	0.05667	3.35	0.20	0.2392	0.0507	0.0388	0.51059	50
39	8	8.55	2	16	36	0.00351	0.10291	1.12	0.16	0.0898	0.0646	0.0339	0.70670	8
40	8	9	2.7	19.5	28	0.00170	0.07684	0.81	0.18	0.0771	0.0407	0.0463	0.65215	30
41	10.9	3.9	9.3	12.5	36	0.00432	0.05156	2.66	0.21	0.1647	0.0543	0.0435	0.69953	10
42	10.9	5.45	10	16	28	0.00182	0.00811	2.48	0.21	0.1587	0.0260	0.0485	0.69092	15
43	10.9	7	2	19.5	28.3	0.00217	0.16769	0.26	0.18	0.0092	0.0399	0.0436	0.72284	5
44	10.9	8.55	2.7	20	32	0.00163	0.16927	0.79	0.13	0.0610	0.0361	0.0211	0.73003	3
45	10.9	9	6	9	35.7	0.00183	0.03455	2.56	0.18	0.0993	0.0515	0.0207	0.70244	9
46	12	3.9	10	19.5	32	0.00290	0.13688	2.24	0.18	0.1789	0.0270	0.0359	0.69858	11
47	12	5.45	2	20	35.7	0.00392	0.27592	0.34	0.14	0.0341	0.0523	0.0265	0.71295	7

Table 10: Continued.

Run	Combined input parameter					New response							GRG	Rank
	I	PON	POFF	DP	SV	MRR	EWR	SR	ROC	θ	CIR	CYL		
48	**12**	**7**	**2.7**	**9**	**36**	**0.00335**	**0.06894**	**1.36**	**0.19**	**0.0014**	**0.0667**	**0.0321**	**0.75302**	**1**
49	12	8.55	6	12.5	28	0.00038	0.01559	1.91	0.20	0.0514	0.0297	0.0332	0.69403	13
50	12	9	9.3	16	28.3	0.00060	0.01717	2.70	0.17	0.1506	0.0101	0.0186	0.72975	4

Table 11: Candidate solution based on the nondominance rank.

S. no	Combined input parameter					New response							GRG	Rank
	I	PON	POFF	DP	SV	MRR	EWR	SR	ROC	θ	CIR	CYL		
1	12	7	2.7	9	36	0.00658	0.00058	1.36	0.19	0.0014	0.0667	0.0321	0.75302	1
2	12	7	4	12	36	0.00219	0.00058	0.77	0.15	0.1098	0.0309	0.0120	0.74252	2
3	10.9	8.55	2.7	20	32	0.00573	0.00079	0.79	0.13	0.0610	0.0361	0.0211	0.73003	3
4	12	9	9.3	16	28.3	0.00610	0.00065	2.70	0.17	0.1506	0.0101	0.0186	0.72975	4
5	10.9	7	2	19.5	28.3	0.00542	0.00010	0.26	0.18	0.0092	0.0399	0.0436	0.72284	5
6	6	6	6	18	36	0.00280	0.00073	1.51	0.15	0.5622	0.0190	0.0094	0.72120	6
7	12	5.45	2	20	35.7	0.00530	0.00059	0.34	0.14	0.0341	0.0523	0.0265	0.71295	7
8	8	8.55	2	16	36	0.00502	0.00083	1.12	0.16	0.0898	0.0646	0.0339	0.70670	8
9	10.9	9	6	9	35.7	0.00648	0.00062	2.56	0.18	0.0993	0.0515	0.0207	0.70244	9
10	10.9	3.9	9.3	12.5	36	0.00450	0.00029	2.66	0.21	0.1647	0.0543	0.0435	0.69953	10
11	12	3.9	10	19.5	32	0.00430	0.00053	2.24	0.18	0.1789	0.0270	0.0359	0.69858	11
12	4	5.45	2.7	12.5	28.3	0.00295	0.00080	0.93	0.29	0.0750	0.0858	0.1034	0.69752	12
13	**12**	**8.55**	**6**	**12.5**	**28**	**0.00652**	**0.00040**	**1.91**	**0.20**	**0.0514**	**0.0297**	**0.0332**	**0.69403**	**13**
14	5.1	5.45	6	19.5	36	0.00248	0.00085	1.78	0.19	0.2230	0.0682	0.0594	0.69307	14
15	10.9	5.45	10	16	28	0.00464	0.00073	2.48	0.21	0.1587	0.0260	0.0485	0.69092	15
16	10	7	2	18	30	0.00255	0.00123	1.15	0.12	0.0877	0.0303	0.0410	0.68945	16
17	12	6	2	20	34	0.00093	0.79000	0.05	0.06	0.0486	0.0557	0.0313	0.68706	17
18	4	8.55	9.3	19.5	35.7	0.00268	0.00116	3.12	0.16	0.3304	0.0486	0.0406	0.68421	18
19	6	5	4	16	34	0.02139	0.00065	0.87	0.38	0.0612	0.1752	0.1549	0.68172	19
20	10	8	4	20	32	0.00207	0.00073	1.17	0.18	0.0951	0.0168	0.0277	0.67799	20
21	4	6	4	14	30	0.00240	0.00032	0.71	0.24	0.0810	0.0491	0.0299	0.67612	21
22	12	5	10	18	32	0.00117	0.00060	0.93	0.21	0.0244	0.0778	0.0307	0.67015	22
23	4	8	8	18	34	0.00444	0.00111	0.56	0.18	0.0848	0.0525	0.0685	0.66312	23
24	6	9	2	14	32	0.00192	0.00069	0.92	0.16	0.0550	0.1465	0.0520	0.66300	24
25	12	8	6	14	28	0.00267	0.00040	1.42	0.24	0.2073	0.0137	0.0231	0.65933	25

Minimization:

$$\text{EWR} = -0.000535 + 0.000106\,I + 0.000065\,\text{PON} - 0.000014\,\text{POFF} - 0.000007\,\text{DP} + 0.000004\,\text{SV}, \tag{18}$$

$$\text{SR} = 0.35 - 0.0242\,I + 0.0076\,\text{PON} + 0.0660\,\text{POFF} + 0.0492\,\text{DP} + 0.0029\,\text{SV}, \tag{19}$$

$$\text{ROC} = 0.118 - 0.00210\,I - 0.00200\,\text{PON} + 0.00010\,\text{POFF} + 0.00320\,\text{DP} + 0.00180\,\text{SV}, \tag{20}$$

$$\theta = 0.367 - 0.03776\,I + 0.0086\,\text{PON} + 0.00444\,\text{POFF} + 0.00327\,\text{DP} - 0.00182\,\text{SV}, \tag{21}$$

$$\text{CIR} = -0.090 + 0.00021\,I - 0.00397\,\text{PON} + 0.00182\,\text{POFF} + 0.00060\,\text{DP} + 0.00459\,\text{SV}, \tag{22}$$

$$\text{CYL} = 0.003 - 0.00411\,I + 0.00295\,\text{PON} + 0.00159\,\text{POFF} - 0.00010\,\text{DP} + 0.00163\,\text{SV}. \tag{23}$$

Table 12: Learner phase–new process variables and objective values after interaction.

S.no	New input parameter					Bounded input parameter					New response							GRG	Rank	Interaction
	I	PON	POFF	DP	SV	I	PON	POFF	DP	SV	MRR	EWR	SR	ROC	θ	CIR	CYL			
1	12	6.75	1.545	6.75	40.4	12	6.75	2	12	36	0.00350	0.13135	0.96	0.18	0.0017	0.0639	0.0300	0.60641	14	1 and 25
2	12.72	6.56	4.66	11.12	38.2	12	6.56	4.66	12	36	0.00315	0.09232	1.68	0.18	0.0573	0.0558	0.0272	0.59075	19	2 and 24
3	11.728	8.671	0.951	20.88	30.9	11.728	8.671	2	20	30.9	0.00124	0.18281	0.53	0.13	0.0270	0.0329	0.0197	0.66722	6	3 and 23
4	12	9.88	9.069	15.12	26.265	12	9	9.069	15.12	28	0.00056	0.02956	2.67	0.17	0.1384	0.0122	0.0212	0.60127	17	4 and 22
5	11.728	7.22	1.34	21.92	27.365	11.728	7.22	2	20	28	0.00169	0.18283	0.21	0.17	0.0004	0.0342	0.0375	0.62493	11	5 and 21
6	5.52	5.56	6.66	17.12	38.2	5.52	5.56	6.66	17.12	36	0.00532	0.05504	2.09	0.20	0.2189	0.0687	0.0592	0.60589	15	6 and 20
7	12.72	5.549	1.34	21.76	36.635	12.72	5.549	2	20	36	0.00367	0.28810	0.34	0.13	0.0263	0.0495	0.0209	0.69926	3	7 and 19
8	8.48	8.55	-0.409	14.46	36.165	8.48	8.55	2	14.46	36	0.00342	0.08616	1.19	0.17	0.0741	0.0658	0.0337	0.61784	13	8 and 18
9	10.768	9.66	7.32	4.16	36.635	10.768	9	7.32	12	36	0.00155	0.00776	2.78	0.16	0.1501	0.0420	0.0138	0.67390	5	9 and 17
10	11.008	3.218	11.709	10.08	39.3	11.008	5	10	12	36	0.00349	0.01693	3.02	0.20	0.1828	0.0481	0.0353	0.59744	18	10 and 16
11	12.132	3.559	10	21.04	34.2	12.132	5	10	20	34.2	0.00249	0.14687	2.44	0.15	0.2007	0.0245	0.0209	0.58206	22	11 and 15
12	3.868	5.45	1.611	9.42	24.065	4	5.45	2	12	28	0.00569	0.03326	0.75	0.29	0.0544	0.0887	0.1061	0.63567	9	12 and 14
13	12	8.891	7.089	14.04	23.6	12	8.891	7.089	14.04	28	0.00576	0.00186	0.96	0.18	0.0869	0.0215	0.0167	0.73367	1	13 and 1
14	4.272	5.109	6.66	22.8	36	4.272	5.109	6.66	20	36	0.00588	0.08795	1.92	0.19	0.2506	0.0696	0.0646	0.62163	12	14 and 2
15	10.9	4.768	12.409	14.24	25.8	10.9	5	10	14.24	28	0.00217	0.01250	2.53	0.23	0.1459	0.0314	0.0544	0.54670	24	15 and 3
16	9.76	6.56	-0.409	18.88	30.935	9.76	6.56	2	18.88	30.935	0.00326	0.16765	0.41	0.18	0.0363	0.0517	0.0467	0.60428	16	16 and 4
17	12.132	5.78	2	20.22	37.135	12.132	5.78	2	20	36	0.00372	0.27516	0.39	0.13	0.0362	0.0510	0.0227	0.68916	4	17 and 5
18	8.5	9.111	10.389	20.16	35.535	8.5	9.111	10	20	35.535	0.00132	0.03507	3.16	0.12	0.2866	0.0246	0.0100	0.70768	2	18 and 6
19	5.28	4.901	4.66	14.24	33.065	5.28	5	4.66	14.24	33.065	0.00577	0.02300	1.49	0.24	0.1386	0.0799	0.0802	0.64285	8	19 and 7
20	10.24	7.879	4.66	21.76	29.8	10.24	7.879	4.66	20	29.8	0.00157	0.12110	1.18	0.16	0.0966	0.0315	0.0324	0.58418	21	20 and 8
21	3.172	5.34	3.34	16.2	26.865	4	5.34	3.34	16.2	28	0.00533	0.00922	0.88	0.27	0.1080	0.0761	0.0980	0.64698	7	21 and 9
22	12.132	5.242	10.231	20.42	29.8	12.132	5.242	10	20	29.8	0.00165	0.10828	2.27	0.17	0.1740	0.0166	0.0314	0.54200	25	22 and 10
23	3.04	8.902	7.34	17.34	35.1	4	8.902	7.34	17.34	35.1	0.00345	0.03616	2.70	0.18	0.2721	0.0572	0.0464	0.58076	23	23 and 11
24	6.24	9.781	1.769	14.66	34.035	6.24	9.781	2	14.66	34.035	0.00307	0.01896	1.33	0.18	0.1024	0.0663	0.0432	0.63513	10	24 and 12
25	12	7.879	6	14.66	28	12	7.879	6	14.66	28	0.00071	0.02914	1.70	0.19	0.0596	0.0280	0.0342	0.58480	20	25 and 13

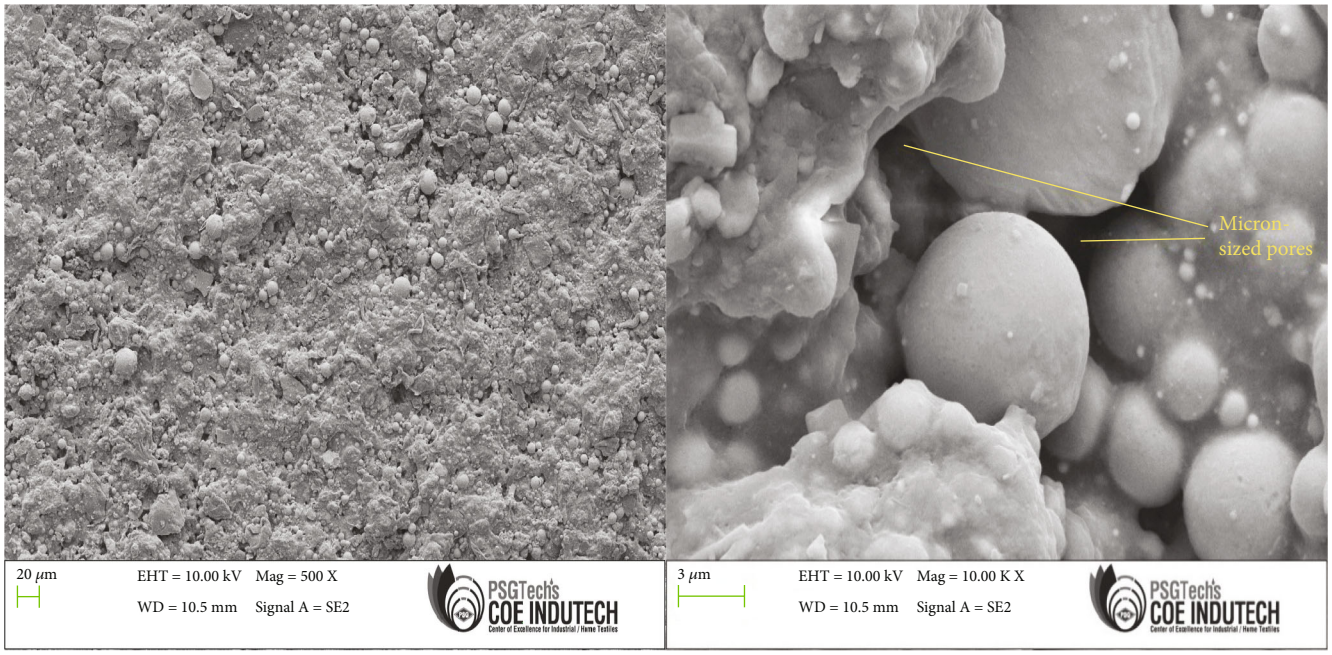

Figure 6: SEM micrographs of machined Si_3N_4–TiN.

Table 13: Comparison of various optimization techniques.

S. no	Output parameters	Taguchi	GRA	TOPSIS	TLBO
	GRG	—	0.75302	0.90578	0.73367
	Setting level	—	I: 12 amps PON: 7 μsec POFF: 4 μsec DP: 12 kg/cm^2 SV: 36 volts ($A_5B_3C_2D_1E_5$)	I: 12 amps PON: 7 μsec POFF: 4 μsec DP: 12 kg/cm^2 SV: 36 volts ($A_5B_3C_2D_1E_5$)	I: 12 amps PON: 8.89 μsec POFF: 7.09 μsec DP: 14.04 kg/cm^2 SV: 28 volts
1	MRR (g/min)	0.00440	0.00219	0.00219	0.00576
2	EWR (g/min)	0.00032	0.00058	0.00058	0.00186
3	SR (μm)	0.56	0.77	0.77	0.96
4	ROC (mm)	0.06	0.15	0.15	0.18
5	θ (deg)	0.0210	0.1098	0.1098	0.0869
6	CIR (mm)	0.0111	0.0309	0.0309	0.0215
7	CYL (mm)	0.0094	0.0120	0.0120	0.0167

Parameter bounds:

$$\text{Pulse current} : 4 \le I \le 12, \tag{24}$$

$$\text{Pulse-on time} : 5 \le \text{PON} \le 9, \tag{25}$$

$$\text{Pulse-off time} : 2 \le \text{POFF} \le 10, \tag{26}$$

$$\text{Dielectric pressure} : 12 \le \text{DP} \le 20, \tag{27}$$

$$\text{Spark gap voltage} : 28 \le \text{SV} \le 36. \tag{28}$$

The TLBO is carried through the accompanying advances.

Step 1. Set the population size, $N_p = 25$.

Step 2. Based on DOE, the design matrix is embraced, and the same is ranked utilizing the GRG as delineated in Table 8.

Step 3 (teacher phase). New solution is generated as delineated in Table 9.

$$X_{\text{new}} = X + r\left(X_{\text{best}} - T_f * X_{\text{mean}}\right), \tag{29}$$

where X_{new} is a recent solution, X is a current solution, r is a random value between 0 and 1, X_{best} is a teacher, T_f is a teaching entity either 1 or 2, and X_{mean} is a mean of the population.

Table 14: Comparison of verification test for various optimization techniques.

S.no	Output parameters		GRA	TOPSIS	TLBO
1	MRR (g/min)	Trial 1	0.00224	0.00199	0.00498
		Trial 2	0.00198	0.00221	0.00591
		Trial 3	0.00227	0.00230	0.00544
		Trial 4	0.00222	0.00204	0.00561
		Trial 5	0.00209	0.00219	0.00553
		Average	**0.00216**	**0.00215**	**0.00549**
2	EWR (g/min)	Trial 1	0.00055	0.00062	0.00092
		Trial 2	0.00061	0.00061	0.00190
		Trial 3	0.00057	0.00056	0.00181
		Trial 4	0.00061	0.00059	0.00199
		Trial 5	0.00062	0.00060	0.00177
		Average	**0.00059**	**0.00060**	**0.00168**
3	SR (μm)	Trial 1	0.77	0.79	0.82
		Trial 2	0.71	0.76	0.9
		Trial 3	0.8	0.81	0.89
		Trial 4	0.79	0.74	0.96
		Trial 5	0.75	0.78	0.95
		Average	**0.76**	**0.78**	**0.90**
4	ROC (mm)	Trial 1	0.14	0.15	0.16
		Trial 2	0.16	0.16	0.19
		Trial 3	0.17	0.16	0.14
		Trial 4	0.15	0.14	0.15
		Trial 5	0.15	0.13	0.19
		Average	**0.15**	**0.15**	**0.17**
5	θ (deg)	Trial 1	0.1089	0.1102	0.0910
		Trial 2	0.1099	0.1099	0.0891
		Trial 3	0.1101	0.1097	0.0852
		Trial 4	0.1089	0.1096	0.0888
		Trial 5	0.1095	0.1092	0.0869
		Average	**0.1095**	**0.1097**	**0.0882**
6	CIR (mm)	Trial 1	0.0308	0.0308	0.0301
		Trial 2	0.0281	0.0314	0.0210
		Trial 3	0.0313	0.0306	0.0202
		Trial 4	0.0304	0.0279	0.0289
		Trial 5	0.0335	0.0328	0.0221
		Average	**0.0308**	**0.0307**	**0.0245**
7	CYL (mm)	Trial 1	0.0121	0.0128	0.0152
		Trial 2	0.0132	0.0123	0.0159
		Trial 3	0.0129	0.0120	0.0182
		Trial 4	0.0115	0.0112	0.0181
		Trial 5	0.0122	0.0128	0.0170
		Average	**0.0124**	**0.0122**	**0.0169**

Step 4. Here, the bounded input factors are joined with the actual parameters taken from design of experiments. Table 10 delineates the combined population.

Step 5. Here, ranks 1 to 25 (50% of higher order rankings) are selected from the combined population table, and the same is optimized through the GRG. Ranks 1 to 25 acquired from the combined population are delineated in Table 11.

Step 6 (learner phase). Creation of new solution is developed by means of a partner response which is haphazardly chosen from the population is delineated in Table 12.

$$X_{\text{new}} = X + r\left(X - X_p\right), \tag{30}$$

where X_p is a partner solution.

Based on the TLBO technique, the global optimal values were identified. The optimal set of input factors are acquired from the learner phase based on the top ranking [1]. This ranking is produced after interaction between parameters as displayed in Table 12. The SEM images of the hole made using optimal machining parameters are delineated in Figure 6. From the micrograph, it is evident that the machined area of the Si_3N_4–TiN ceramic matrix composite workpiece exhibits good surface finish.

3.5. Verification Test. The GRG for different optimization methods is calculated for electrodischarge machining of Si_3N_4–TiN ceramic matrix composite workpiece. A point by point correlation is made for the GRG acquired from joint optimization techniques and is outlined in Table 13. Finally, a confirmatory experiment was done for the final TLBO optimized values, and the outcomes are great in contention. Table 14 portrays the outcomes obtained for optimal input machining factors.

4. Conclusions

The input factors influencing electrodischarge machining of adsorbed Si_3N_4–TiN workpiece using cylindrical-shaped W-Cu electrode were examined. The experimental runs for directing the experiments were arranged utilizing statistical tool by design of experiments methodology. The disparate mixture of input factors like I, PON, POFF, DP, and SV is chosen in this research. The outputs like MRR, EWR, SR, ROC, θ, CIR, and CYL are determined. Here, various optimization methodologies like Taguchi methodology, grey relational analysis, TOPSIS, and TLBO are engaged to obtain the combination of optimized factors to increase material removal rate and to decrease EWR, SR, taper angle, ROC, circularity, and cylindricity. From the experimental results and calculations, the accompanying conclusions were obtained:

(i) The outcomes determined for grey relational analysis and TOPSIS are comparative. The best output factors are obtained for I = 12 amps, PON = 7 μsec, POFF = 4 μsec, DP = 12 kg/cm^2, and SV = 36 volts ($A_5B_3C_2D_1E_5$).

(ii) The execution of GRA coupled with TLBO a global optimization technique gave the preferred outcomes over that of other methodologies. The accompanying

combination was achieved from GRA coupled with TLBO algorithm I = 12 amps, PON = 8.89 μsec, POFF = 7.09 μsec, DP = 14.04 kg/cm^2, and SV = 28 volts.

4.1. Future Scopes of the Research

(i) This study can be further extended for nanocomposites and microstructure studies on machined surface of adsorbed Si_3N_4–TiN composites.

(ii) Other shape of electrodes like rectangle, hexagon, and octagon can be employed.

(iii) Furthermore, in the future, different electrode materials can be employed to characterize the surface integrity, fatigue performance, and dry sliding wear behaviour of adsorbed Si_3N_4–TiN. Also, different polishing methods can be imparted for better surface finish and fatigue life, higher wear resistance, and microhardness.

(iv) Optimization techniques like genetic algorithm, simulated annealing, particle swarm optimization, and ant bee colony optimization can be employed to find out significant parameters.

Nomenclature

CIR:	Circularity
CLE:	Composite laminated electrode
CYL:	Cylindricity
DOE:	Design of experiments
DP:	Dielectric pressure
EDM:	Electrical discharge machining
EWR:	Electrode wear rate/electrode erosion rate
GA:	Genetic algorithm
GRA:	Grey relational analysis
GRC:	Grey relational coefficient
GRG:	Grey relational grade
I:	Pulse current
MCDM:	Multicriteria decision-making
MRR:	Material removal rate
POFF:	Pulse-off time
PON:	Pulse-on time
PSO:	Particle swarm optimization
ROC:	Radial overcut
Si_3N_4–TiN:	Silicon nitride–titanium nitride
SI:	Similarity index
SR:	Surface roughness
SV:	Spark gap voltage
TLBO:	Teaching-learning-based optimization
TOPSIS:	Technique for order of preference by similarity to ideal solution
θ:	Taper angle.

Data Availability

The data were within this article.

Conflicts of Interest

The authors declare that they have no conflict of interest.

References

[1] V. P. Srinivasan, P. K. Palani, and S. Balamurugan, "Experimental investigation on EDM of Si_3N_4-TiN using grey relational analysis coupled with teaching-learning-based optimization algorithm," *Ceramics International*, vol. 47, no. 13, pp. 19153–19168, 2021.

[2] Z. Zhang, Y. Zhang, W. Ming, Y. Zhang, C. Cao, and G. Zhang, "A review on magnetic field assisted electrical discharge machining," *Journal of Manufacturing Processes*, vol. 64, pp. 694–722, 2021.

[3] S. Suresh Kumar, T. Varol, A. Canakci, S. Thirumalai Kumaran, and M. Uthayakumar, "A review on the performance of the materials by surface modification through EDM," *International Journal of Lightweight Materials and Manufacture*, vol. 4, no. 1, pp. 127–144, 2021.

[4] S. Dasa, U. Acharya, S. V. V. N. Siva Rao, S. Paul, and B. S. Roy, "Assessment of the surface characteristics of aerospace grade AA6092/17.5 SiCp-T6 composite processed through EDM," *CIRP Journal of Manufacturing Science and Technology*, vol. 33, pp. 123–132, 2021.

[5] S. N. Grigoriev, K. Hamdy, M. A. Volosova, A. A. Okunkov, and S. V. Fedorov, "Electrical discharge machining of oxide and nitride ceramics: a review," *Materials & Design*, vol. 209, article 109965, 2021.

[6] S. Kumar, R. Singh, T. P. Singh, and B. L. Sethi, "Surface modification by electrical discharge machining: a review," *Journal of Materials Processing Technology*, vol. 209, no. 8, pp. 3675–3687, 2009.

[7] J. T. Philip, J. Mathew, and B. Kuriachen, "Transition from EDM to PMEDM - impact of suspended particulates in the dielectric on Ti6Al4V and other distinct material surfaces: a review," *Journal of Manufacturing Processes*, vol. 64, pp. 1105–1142, 2021.

[8] K. Jiang, W. Xiaoyu, J. Lei et al., "Investigation on the geometric evolution of microstructures in EDM with a composite laminated electrode," *Journal of Cleaner Production*, vol. 298, article 126765, 2021.

[9] S. Das, S. Paul, and B. Doloi, "A gap-active electrical discharge machining (GA-EDM) to rectify the textural defects of the processed surface," *Journal of Manufacturing Processes*, vol. 64, pp. 594–605, 2021.

[10] S. Chakraborty, V. Dey, and S. K. Ghosh, "A review on the use of dielectric fluids and their effects in electrical discharge machining characteristics," *Precision Engineering*, vol. 40, pp. 1–6, 2014.

[11] B. Singaravel, K. C. Shekar, G. G. Reddy, and S. D. Prasad, "Experimental investigation of vegetable oil as dielectric fluid in Electric discharge machining of Ti-6Al-4V," *Ain Shams Engineering Journal*, vol. 11, no. 1, pp. 143–147, 2020.

[12] R. V. Rao, V. J. Savsani, and D. P. Vakharia, "Teaching-learning-based optimization: a novel method for constrained mechanical design optimization problems," *Computer-Aided Design*, vol. 43, no. 3, pp. 303–315, 2011.

[13] Y. Ma, X. Zhang, J. Song, and L. Chen, "A modified teaching-learning-based optimization algorithm for solving optimization problem," *Knowledge-Based Systems*, vol. 212, no. 5, article 106599, 2021.

[14] S. Vitayasak and P. Pongcharoen, "Performance improvement of teaching-learning-based optimisation for robust machine layout design," *Expert Systems with Applications*, vol. 98, pp. 129–152, 2018.

[15] A. Baykasoğlu, A. Hamzadayi, and S. Y. Köse, "Testing the performance of teaching-learning based optimization (TLBO) algorithm on combinatorial problems: flow shop and job shop scheduling cases," *Information Sciences*, vol. 276, pp. 204–218, 2014.

[16] A. Semnani, M. Ostadhassan, X. Yungui, M. Sharifi, and B. Liu, "Joint optimization of constrained well placement and control parameters using teaching-learning based optimization and an inter-distance algorithm," *Journal of Petroleum Science and Engineering*, vol. 203, article 108652, 2021.

[17] N. Ahmad and H. Sueyoshi, "Properties of Si_3N_4-TiN composites fabricated by spark plasma sintering by using a mixture of Si_3N_4 and Ti powders," *Ceramics International*, vol. 36, no. 2, pp. 491–496, 2010.

[18] N. Ahmad and H. Sueyoshi, "Microstructure and mechanical properties of silicon nitride-titanium nitride composites prepared by spark plasma sintering," *Materials Research Bulletin*, vol. 46, no. 3, pp. 460–463, 2011.

[19] N. Ahmad and H. Sueyoshi, "Densification and mechanical properties of electroconductive Si_3N_4–based composites prepared by spark plasma sintering," *Sains Malaysiana*, vol. 41, no. 8, pp. 1005–1009, 2012.